

Cite this: *Chem. Sci.*, 2023, 14, 7215



All publication charges for this article have been paid for by the Royal Society of Chemistry

Received 13th March 2023
Accepted 4th June 2023

DOI: 10.1039/d3sc01346d

rsc.li/chemical-science

A translationally active ligand based on a [2]rotaxane molecular shuttle with a 2,2'-bipyridyl core†

Ayan Dhara, Anton Dmitrienko, Rahaf N. Hussein, Ariel Sotomayor, Benjamin H. Wilson  and Stephen J. Loeb *

A rigid H-shaped, [2]rotaxane molecular shuttle comprised of an axle containing two benzimidazole recognition sites and a central 2,2'-bipyridyl (bipy) group interlocked with a 24-crown-8 (24C8) wheel was synthesized using a threading followed by stoppering protocol. The central bipy chelating unit was shown to act as a speed bump that raised the barrier to shuttling for the [2]rotaxane. Coordination of a PtCl₂ moiety to the bipy unit in a square planar geometry created an insurmountable steric barrier to shuttling. Addition of one equivalent of NaB(3,5-(CF₃)₂C₆H₃)₄ removed one of the chloride ligands allowing for translation of the crown ether along the axle into the coordination sphere of the Pt(II) centre but full shuttling of the crown ether could not be activated. In contrast, addition of Zn(II) ions in a coordinating solvent (DMF) allowed shuttling to occur using a ligand exchange mechanism. DFT calculations showed this likely occurs *via* coordination of the 24C8 macrocycle to the Zn(II) centre bound to the bipy chelate. This interplay of the rotaxane axle and wheel components is an example of a translationally active ligand that utilises the large amplitude displacement of a macrocycle along an axle in a molecular shuttle to access ligand coordination modes not possible with conventional ligand designs.

Introduction

The design of purpose-built multidentate ligands has extensive history in the areas of catalysis,^{1–5} ion sequestration^{6–9} and bioinorganic chemistry.^{10–12} Rotaxanes which involve separate axle and macrocyclic wheel components held together by a mechanical bond offer a way to bring disparate donor groups together that might not be possible, or more difficult to accomplish with a single component molecule.^{13,14} Although metal ions have been utilised to template rotaxane formation¹⁵ – both passively and actively – and used to induce switching between co-conformations,^{16–19} exploration of the mechanical bond as a fundamental feature of ligand design is limited.^{13,20} In particular, the rotational and translational dynamics of rotaxanes are features not available with single component designs and their application in transition metal chemistry is rare.^{15,21}

We recently explored the idea of using the rotational motion of a macrocycle about a rigid chelating axle to demonstrate how

different binding modes of the rotaxane ligand can be “dialled-up” by rotating the macrocycle and how this affects metal ion binding and selectivity.^{22,23} Herein, we look at the concept of including large amplitude translation of a macrocycle along a rigid chelating axle into a ligand and investigate how this might affect the metal ion coordination and shuttling dynamics of such a system. The basic design components employed herein, an axle with a bipyridine chelate and a crown ether macrocycle, as well as the resulting interlocked [2]rotaxane ligand are shown in Fig. 1. We were interested in shedding light on the following questions: (i) how would the presence of the bipyridine N-atoms affect shuttling of the macrocycle in the free ligand, (ii) could the crown ether be used as a weak donor to a metal ion bound to the bipy chelate and (iii) was it possible for the macrocyclic wheel unit to undergo shuttling in the presence of a coordinated metal ion, perhaps by utilizing coordination to the metal and concomitant ligand exchange?

Results and discussion

Synthesis, and characterization of the [2]rotaxane ligand

The [2]rotaxane molecular shuttle ligand **4** was prepared as described in Scheme 1. Initially, diamine **1** was condensed with an excess of bipyridine-dialdehyde **2** to yield T-shaped benzimidazole **3** in 68% yield. Protonation of **3** with HBF₄ to give [3-H]BF₄ provided a benzimidazolium recognition site that, when

Department of Chemistry and Biochemistry, University of Windsor, Windsor, ON, N9B 3P4, Canada. E-mail: loeb@uwindsor.ca

† Electronic supplementary information (ESI) available: Experimental details describing the synthesis and characterization of all new compounds including solution NMR assignments, VT and 2D NMR experiments, crystal structures. CCDC 2248267–2248268. For ESI and crystallographic data in CIF or other electronic format see DOI: <https://doi.org/10.1039/d3sc01346d>



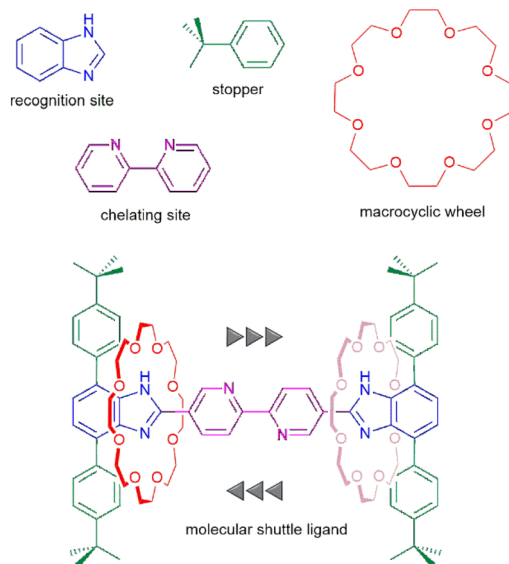


Fig. 1 Design of a translationally active ligand based on a [2]rotaxane molecular shuttle showing the individual components and assembled ligand.

combined with **24C8** in CHCl_3 yielded the [2]pseudorotaxane $[3\text{-H}\text{-}24\text{C8}]\text{BF}_4$. This was followed by a further condensation between the remaining aldehyde group of $[3\text{-H}\text{-}24\text{C8}]\text{BF}_4$ and diamine **1** to give [2]rotaxane **4** in 67% yield. **4** was fully characterised by ^1H and ^{13}C NMR spectroscopy as well as HR-ESI MS and single crystal X-ray diffraction. Solution data are available in the ESI (see Fig. S8–S10[†]) and the solid-state structure of **4** is shown in Fig. 2.

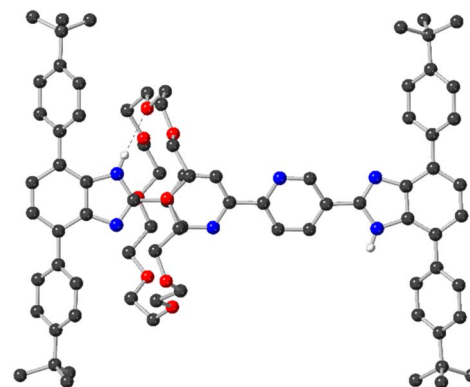
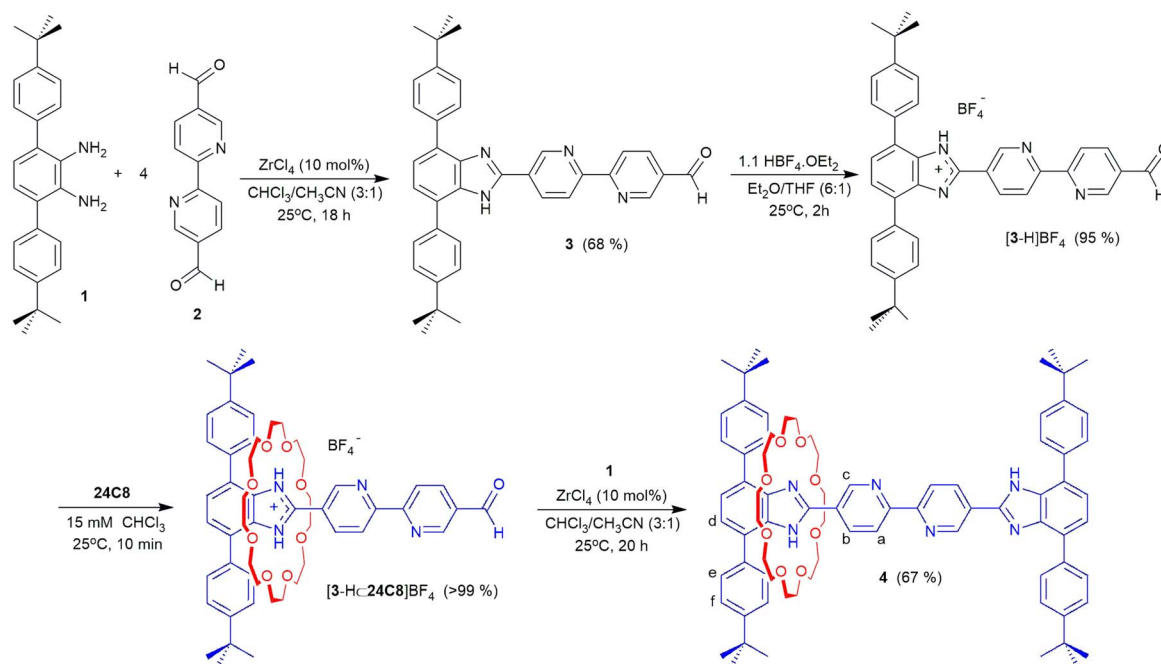


Fig. 2 Single-crystal X-ray structure of [2]rotaxane ligand **4**. Colour key: C dark grey, N blue, H white; covalent bonds grey, H-bonds dashed. All H atoms except those bonded to N atoms were omitted for clarity.

The X-ray structure of **4** shows that the crown ether prefers to reside at one of the benzimidazole recognition sites where it is held in place by hydrogen bonding between one of the axle benzimidazole NH groups and crown ether O-atoms. The overall structure is very similar to a related neutral rotaxane in which the central bipyridine unit is a single phenyl group.²⁴ Importantly, it is clear from the structure that the benzimidazole recognition site and accompanying crown ether do not block access to the chelating bipyridine group.

Shuttling of the [2]rotaxane ligand

The ^1H NMR spectrum of **4** (see ESI, Fig. S8[†]) shows a single set of averaged resonances for complexed and uncomplexed axle



Scheme 1 Synthesis of [2]rotaxane molecular shuttle ligand **4**. Labels for ^1H NMR peak assignments are shown for **4**.



protons indicating that the **24C8** wheel is shuttling between the two benzimidazole recognition sites at a rate that is faster than the NMR timescale. Variable temperature ^1H NMR spectra in CD_2Cl_2 (see ESI, Fig. S9 \dagger) were recorded for **4** and used to determine the rate of translational motion. The observed shuttling rate of 61.2 s^{-1} ($\Delta G^\ddagger = 15.1\text{ kcal mol}^{-1}$) is significantly slower than that observed for a similar system with a biphenyl unit and dibenzo[24]crown-8,²⁴ $6.2 \times 10^3\text{ s}^{-1}$, ($\Delta G^\ddagger = 9.0\text{ kcal mol}^{-1}$) indicating that the presence of the bipyridine group on the axle acts as a speed bump for shuttling. This was attributed to the electronic repulsion between the bipy N-atoms and crown ether O-atoms which significantly raises the barrier to translational motion of the wheel along the axle.

Coordination of rotaxane to Pt(II)

Initially, the substitutionally inert PtCl_2 fragment was chosen for chelation to the bipy site of the axle as square planar complexes of the type $[\text{PtCl}_2(\text{bipy})]$ are well known. In addition, it was reasoned that this would be a good base-line structure as it was very unlikely to involve coordination of the crown ether wheel component of the rotaxane. This was accomplished by reacting $[\text{PtCl}_2(\text{DMSO})_2]$ and **4** in $\text{CH}_3\text{CN}/\text{CHCl}_3$ (10/1) at $100\text{ }^\circ\text{C}$ for 16 h. The solvent was removed from the resulting yellow solution, and the precipitate washed with a basic solution of acetonitrile to yield $[\text{PtCl}_2(\mathbf{4})]$ in 55% isolated yield.

Fig. 3a shows the ^1H NMR spectrum of $[\text{PtCl}_2(\mathbf{4})]$. Coordination of PtCl_2 to the central bipy chelate site results in desymmetrisation of the [2]rotaxane such that separate sets of

resonances are observed for the two different halves of the molecule *i.e.*, with and without crown ether present. Thus, the PtCl_2 fragment acts as a steric barrier to translation of the crown ether. The use of metal ion coordination to arrest wheel translation of a molecular shuttle has been accomplished previously but involved bringing axles from two separate rotaxanes together to bind a metal ion and could only be reversed by removal of the metal ion using exchange resin.²⁵ In order to investigate whether the crown ether could participate in binding to the Pt(II) centre, $[\text{PtCl}_2(\mathbf{4})]$ was reacted with one equivalent of $\text{Na}[\text{BARF}]$ ($\text{BARF} = \text{B}(3,5\text{-}(\text{CF}_3)_2\text{C}_6\text{H}_3)_4$) in CH_2Cl_2 . Fig. 3b shows the ^1H NMR spectrum of the complex $[\text{PtCl}(\mathbf{4})][\text{BARF}]$. Changes in the spectrum infer removal of a chloride ion and coordination of the **24C8** wheel to the Pt(II) centre (see ESI, Fig. S18 \dagger).

Attempts to remove the remaining chloride ion using a further equivalent of $\text{Na}[\text{BARF}]$ were unsuccessful (see ESI, Fig. S19 \dagger). This can be attributed to the fact that the **24C8** macrocycle is not capable of occupying two coordination sites at the square planar Pt(II) centre while it is restricted to an orientation perpendicular to the axle on account of its participation in the mechanical bond.

To further investigate the degree to which the crown ether could coordinate to the Pt(II) centre of $[\text{PtCl}_2(\mathbf{4})]$, a sample was dissolved in DMSO-d_6 and evidence of exchange between the two benzimidazole resonances probed by EXSY (EXchange Spectroscopy) NMR experiments. It was hypothesised that it might be possible for the **24C8** wheel to shuttle from one recognition site to the other using a series of steps involving chloride ion, solvent exchange²⁶ and coordination of the **24C8** macrocycle to the Pt centre. However, no evidence of wheel exchange between the recognition sites was observed even at increased temperatures (see ESI, Fig. S22 \dagger). The lack of shuttling was attributed to the awkward combination of a square planar coordination environment parallel to the axle and the restricted orientation of the macrocyclic due to its participation in the mechanical bond.

Coordination of rotaxane to Zn(II)

Since the relative orientation of the square planar geometry dictated by the bipy chelate and the track of the molecular shuttle were not conducive to ligand exchange assisted shuttling, it was reasoned that employing a metal centre without this geometric restriction might alleviate the problem.²⁷ To test this hypothesis, one equivalent of ZnCl_2 was added to a solution of **4** in CH_2Cl_2 at room temperature similar to the approach taken with coordination to Pt(II). Unfortunately, the ^1H NMR spectrum of the mixture showed that the resulting Zn(II) complex had been converted to the mono-protonated species in which the crown ether binds solely to the newly created benzimidazolium group (see ESI, Fig. S23 \dagger). Such ease of protonation of basic groups when encircled by a crown ether as part of a rotaxane is well known^{28–31} and is probably promoted by adventitious water in the presence of Lewis acidic Zn(II) ions.^{32,33} Attempts to deprotonate the complex with moderately strong bases such as proton sponge were unsuccessful, and the use of stronger bases

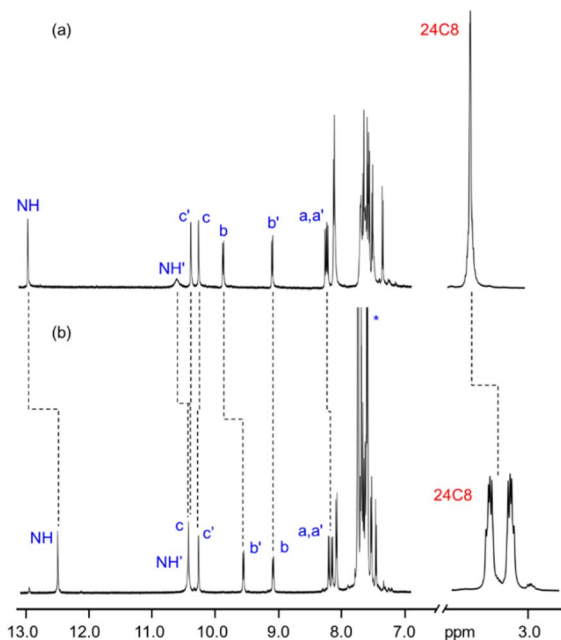


Fig. 3 ^1H NMR spectra of (a) $[\text{PtCl}_2(\mathbf{4})]$ and (b) $[\text{PtCl}(\mathbf{4})][\text{BARF}]$ in CD_2Cl_2 . See Scheme 1 for labels, H-atoms labelled prime (e.g., a') are from parts of the axle not interacting with **24C8**. * indicates peaks due to the BARF anion.



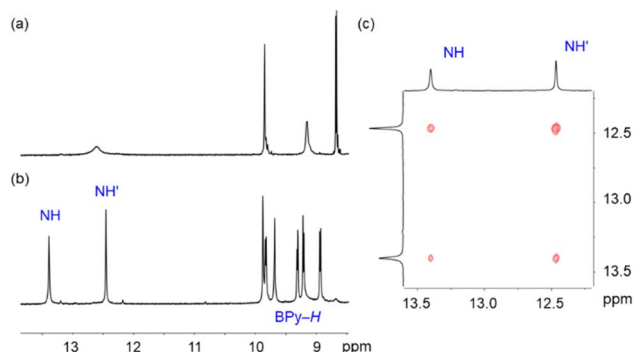
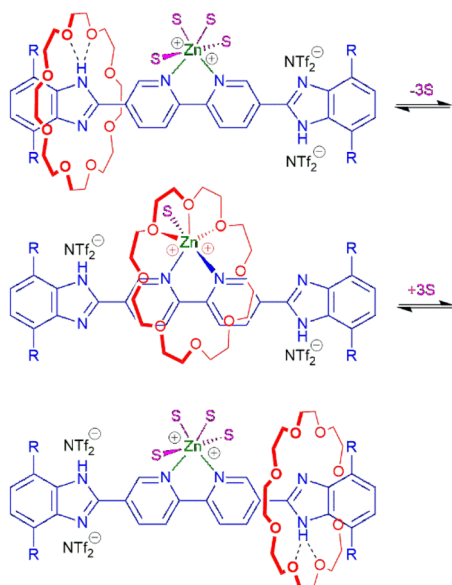


Fig. 4 ^1H NMR spectra in DMF-d_7 of (a) **4**, (b) $[\text{Zn}(\text{DMF})_4(\mathbf{4})][\text{NTf}_2]_2$ and (c) partial EXSY spectrum showing exchanging NH peaks of $[\text{Zn}(\text{DMF})_4(\mathbf{4})][\text{NTf}_2]_2$.

such as hydroxide ion resulted in decomposition of the complex.

After further testing numerous solvents and counterions, it was discovered that the addition of $[\text{Zn}(\text{NTf}_2)_2]$ to **4** in DMF produced a neutral Zn(II) complex formulated as $[\text{Zn}(\text{DMF})_4(\mathbf{4})][\text{NTf}_2]_2$. The ^1H NMR spectra of **4** and the Zn(II) complex are shown in Fig. 4. Similar to the Pt(II) complexes, the ^1H NMR spectrum of $[\text{Zn}(\text{DMF})_4(\mathbf{4})][\text{NTf}_2]_2$ indicates that the **24C8** macrocycle resides at one of the benzimidazole recognition sites resulting in the observation of complexed and uncomplexed environments for each axle H-atom.

Interestingly, in contrast to $[\text{PtCl}_2(\mathbf{4})]$ in DMSO which showed no evidence of shuttling, the EXSY spectrum (see Fig. 4c and ESI Fig. S33 †) of $[\text{Zn}(\text{DMF})_4(\mathbf{4})][\text{NTf}_2]_2$ in DMF-d_7 exhibited cross peaks indicative of benzimidazole NH exchange and molecular shuttling. Scheme 2 outlines the presumed ligand-solvent-**24C8** exchange that occurs to allow the required



Scheme 2 Proposed mechanism to promote shuttling of rotaxane wheel *via* ligand and solvent (S) exchange for $[\text{Zn}(\text{S})_4(\mathbf{4})][\text{NTf}_2]_2$.

translational shuttling motion. The key difference is that coordination to Zn(II) allows for an intermediate geometry where the crown ether can bind easily to the Zn(II) ions as it transits from one end of the axle to the other. These measurements produced a shuttling rate of 2.2 s^{-1} ($\Delta G^\ddagger = 17.0 \text{ kcal mol}^{-1}$) which is slower than that for the free ligand **4**, presumably due to the Zn(II) coordination. Since the rate is dependent upon solvent exchange, it would be reasonable to assume that the rate of this type of shuttling would be dependent upon the solvent used. Unfortunately, this could not be verified with this system as only the DMF solutions studied were amenable to these measurements.

DFT calculations were used to provide insight into the interaction between the Zn(II) centre and the rotaxane during the shuttling event. Fig. 5 shows a DFT calculated structure (see ESI † for details) of the exchange intermediate in which three of the crown ether oxygen atoms, the bipyridine chelate and a molecule of DMF are coordinated to the Zn(II) centre in an octahedral geometry. We have previously observed the coordination of three consecutive O-atoms of the macrocycle in this fashion when investigating the coordination of Ag(I) ions to a rotationally active rotaxane containing a bis(benzimidazole) chelate and a 24-membered crown ether.²³

Finally, slow evaporation of a 1 : 1 mixture of Zn(II) ions and rotaxane **4** afforded single crystals that allowed identification of an ML_2 complex, $[\text{Zn}(\mathbf{4})_2(\text{DMF})(\text{H}_2\text{O})][\text{NTf}_2]_2$, in which two bipyridine ligands from two different rotaxane molecules were able to coordinate to a single Zn(II) centre in an octahedral geometry; the single crystal X-ray structure is shown in Fig. 6. It is interesting that two of these bulky rotaxanes are capable of coordinating to the same metal atom and it should be noted this arrangement, in principle, prevents shuttling of the crown ether component. Although it was not possible to directly observe this complex *via* ^1H NMR spectroscopy at varying M : L ratios or concentrations (see ESI, Fig. S31 and S32 †), it is likely that this complex is present in solution with $[\text{Zn}(\text{DMF})_4(\mathbf{4})][\text{NTf}_2]_2$ at lower M : L ratios.

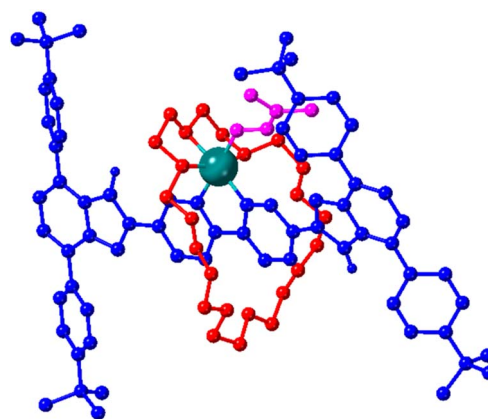


Fig. 5 DFT calculated structure of proposed octahedral intermediate adopted during shuttling of **24C8** macrocycle of $[\text{Zn}(\text{DMF})_4(\mathbf{4})][\text{NTf}_2]_2$ in DMF solution; see Scheme 2 (centre). Axle blue, wheel red, DMF pink, Zn teal. All H atoms except those bonded to imidazole N atoms were omitted for clarity.



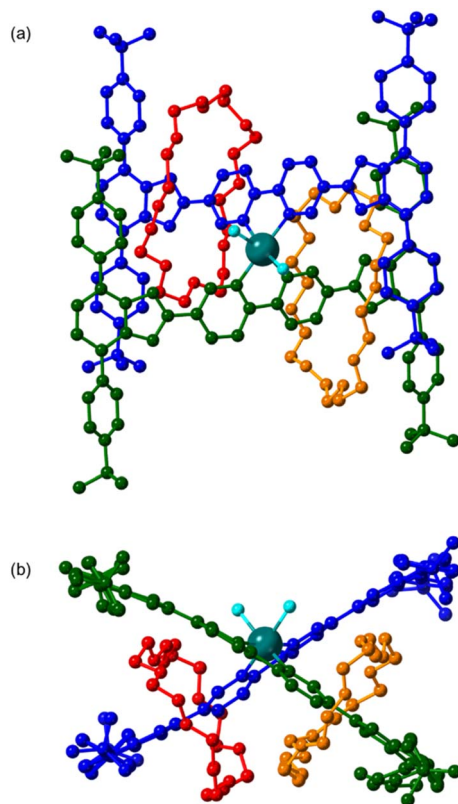


Fig. 6 Single-crystal-X-ray structure of the complex formed from a solution with a 1 : 1 Zn to 4 ratio; $[\text{Zn}(\text{4})_2(\text{DMF})(\text{H}_2\text{O})][\text{NTf}_2]_2$. (a) Side view emphasizing the octahedral coordination geometry at Zn(II). (b) Top view showing the relative positions of the crown ether macrocycles on the rotaxane ligands. Rotaxanes are coloured blue axle with red wheel and green axle with orange wheel. Only the O-atoms of the coordinated DMF and water molecules are shown for clarity. Anions are not shown. All H-atoms are omitted for clarity.

Conclusions

We have reported the design and synthesis of a new molecular shuttle containing a chelating bipy unit. As previously observed, coordination of a metal centre to a chelate site on a molecular shuttle axle can block the translational motion²⁶ and act as a brake to shuttling as was observed herein with Pt(II). However, it was discovered that the use of a metal centre such as Zn(II) allowed for the shuttling of a macrocycle along the axle to occur via a process involving wheel coordination and ligand exchange. This study is the first to: (i) delineate the concept of a translationally active ligand, (ii) demonstrate molecular shuttling aided by ligand coordination, and (iii) show that shuttling can be controlled (on or off) by tuning the coordination geometry – octahedral versus square planar – of a bound metal. More generally, the ability to transiently involve a weak donor (e.g., ether O-atom) from a mechanically bound macrocycle in the coordination environment of a reactive metal centre might be useful in catalysis and the discovery of a new way to control the translational motion of the wheel in a molecular shuttle expands the scope of utilizing mechanically interlocked

molecules as ligands in traditional coordination and organometallic chemistry.

Data availability

All associated data are in ESI† or deposited with CCDC.

Author contributions

Conceptualization – S. J. L.; investigation – A. D. 1, A. S., R. N. H., and B. H. W.; formal analysis – A. D. 1, and A. D. 2 (crystallography); writing – original draft, S. J. L.; writing – review & editing, A. D. 1, A. D. 2, and S. J. L.; funding acquisition, S. J. L.

Conflicts of interest

There are no conflicts to declare.

Acknowledgements

This research was supported by the Natural Sciences and Engineering Research Council of Canada (Discovery Grant No. 101694 to SJL). A. D. 1 and S. J. L. acknowledge M. Revington for technical assistance with 2D NMR spectroscopy experiments and Prof. J. Rawson for helpful discussions related to our DFT calculations.

Notes and references

- V. T. Annibale and D. Song, Multidentate actor ligands as versatile platforms for small molecule activation and catalysis, *RSC Adv.*, 2013, **3**, 11432–11449.
- E. C. Constable and C. E. Housecroft, The Early Years of 2,2'-Bipyridine—A Ligand in Its Own Lifetime, *Molecules*, 2019, **24**, 3951.
- M. D. Sampson, A. D. Nguyen, K. A. Grice, C. E. Moore, A. L. Rheingold and C. P. Kubiak, Manganese Catalysts with Bulky Bipyridine Ligands for the Electrocatalytic Reduction of Carbon Dioxide: Eliminating Dimerization and Altering Catalysis, *J. Am. Chem. Soc.*, 2014, **136**, 5460–5471.
- V. A. Malkov and P. Kocovsky, Chiral Bipyridine Derivatives in Asymmetric Catalysis, *Curr. Org. Chem.*, 2003, **7**, 1737–1757.
- E. Peris and R. H. Crabtree, Key factors in pincer ligand design, *Chem. Soc. Rev.*, 2018, **47**, 1959–1968.
- A. E. V. Gorden, J. Xu, K. N. Raymond and P. Durbin, Rational Design of Sequestering Agents for Plutonium and Other Actinides, *Chem. Rev.*, 2003, **103**, 4207–4282.
- D. L. White, P. W. Durbin, N. Jeung and K. N. Raymond, Specific sequestering agents for the actinides. 16. Synthesis and initial biological testing of polydentate oxohydroxypyridinecarboxylate ligands, *J. Med. Chem.*, 1988, **31**, 11–18.
- C. J. Carrano and K. N. Raymond, Ferric ion sequestering agents. 2. Kinetics and mechanism of iron removal from



- transferrin by enterobactin and synthetic tricatechols, *J. Am. Chem. Soc.*, 1979, **101**, 5401–5404.
- 9 I. Turcot, A. Stintzi, J. Xu and K. N. Raymond, Fast biological iron chelators: kinetics of iron removal from human diferric transferrin by multidentate hydroxypyridonates, *JBIC, J. Biol. Inorg. Chem.*, 2000, **5**, 634–641.
- 10 K. Degtyarenko, Bioinorganic motifs: towards functional classification of metalloproteins, *Bioinformatics*, 2000, **16**, 851–864.
- 11 J. M. Berg, *Principles of bioinorganic chemistry*, University Science Books, 1994.
- 12 A. C. Hachey, D. Havrylyuk and E. C. Glazer, Biological activities of polypyridyl-type ligands: implications for bioinorganic chemistry and light-activated metal complexes, *Curr. Opin. Chem. Biol.*, 2021, **61**, 191–202.
- 13 M. Cirulli, A. Kaur, J. E. M. Lewis, Z. Zhang, J. A. Kitchen, S. M. Goldup and M. M. Roessler, Rotaxane-Based Transition Metal Complexes: Effect of the Mechanical Bond on Structure and Electronic Properties, *J. Am. Chem. Soc.*, 2019, **141**, 879–889.
- 14 S. J. Loeb, Rotaxanes as ligands: from molecules to materials, *Chem. Soc. Rev.*, 2007, **36**, 226–235.
- 15 J. E. M. Lewis, P. D. Beer, S. J. Loeb and S. M. Goldup, Metal ions in the synthesis of interlocked molecules and materials, *Chem. Soc. Rev.*, 2017, **46**, 2577–2591.
- 16 C. O. Dietrich-Buchecker, J. P. Sauvage and J. P. Kintzinger, Une nouvelle famille de molecules : les metallo-catenanes, *Tetrahedron Lett.*, 1983, **24**, 5095–5098.
- 17 J.-P. Sauvage, Transition metal-complexed catenanes and rotaxanes as molecular machine prototypes, *Chem. Commun.*, 2005, 1507–1510.
- 18 A. I. Prikhod'ko, F. Durolo and J.-P. Sauvage, Iron(II)-Templated Synthesis of [3]Rotaxanes by Passing Two Threads through the Same Ring, *J. Am. Chem. Soc.*, 2008, **130**, 448–449.
- 19 J.-C. Chambron, J.-P. Collin, V. Heitz, D. Jouvenot, J.-M. Kern, P. Mobian, D. Pomeranc and J.-P. Sauvage, Rotaxanes and Catenanes Built around Octahedral Transition Metals, *Eur. J. Org. Chem.*, 2004, **2004**, 1627–1638.
- 20 M. Denis and S. M. Goldup, The active template approach to interlocked molecules, *Nat. Rev. Chem.*, 2017, **1**, 0061.
- 21 I. Poleschak, J.-M. Kern and J.-P. Sauvage, A copper-complexed rotaxane in motion: pirouetting of the ring on the millisecond timescale, *Chem. Commun.*, 2004, 474–476.
- 22 G. Baggi and S. J. Loeb, Rotationally Active Ligands: Dialing-Up the Co-conformations of a [2]Rotaxane for Metal Ion Binding, *Angew. Chem., Int. Ed.*, 2016, **55**, 12533–12537.
- 23 G. Baggi and S. J. Loeb, Rotationally Active Ligands: Dialing-Up Multiple Interlocked Co-Conformations for Silver(I) Coordination, *Chem.–Eur. J.*, 2017, **23**, 14163–14166.
- 24 G. Gholami, K. Zhu, G. Baggi, E. Schott, X. Zarate and S. J. Loeb, Influence of axle length on the rate and mechanism of shuttling in rigid H-shaped [2]rotaxanes, *Chem. Sci.*, 2017, **8**, 7718–7723.
- 25 L. Jiang, J. Okano, A. Orita and J. Otera, Intermittent Molecular Shuttle as a Binary Switch, *Angew. Chem., Int. Ed.*, 2004, **43**, 2121–2124.
- 26 R. G. Pearson, H. B. Gray and F. Basolo, Mechanism of Substitution Reactions of Complex Ions. XVI. Exchange Reactions of Platinum(II) in Various Solvents, *J. Am. Chem. Soc.*, 1960, **82**, 787–792.
- 27 Other cations were investigated (Li^+ , Ag^+ , Cu^+) but resulted in complex mixtures which included significant amounts of $[\text{4-H}]^+$.
- 28 K. Nakazono and T. Takata, Neutralization of a sec-Ammonium Group Unusually Stabilized by the “Rotaxane Effect”: Synthesis, Structure, and Dynamic Nature of a “Free” sec-Amine/Crown Ether-Type Rotaxane, *Chem.–Eur. J.*, 2010, **16**, 13783–13794.
- 29 K. Zhu, V. N. Vukotic and S. J. Loeb, Molecular Shuttling of a Compact and Rigid H-Shaped [2]Rotaxane, *Angew. Chem., Int. Ed.*, 2012, **51**, 2168–2172.
- 30 K. Zhu, C. A. O'Keefe, V. N. Vukotic, R. W. Schurko and S. J. Loeb, A molecular shuttle that operates inside a metal–organic framework, *Nat. Chem.*, 2015, **7**, 514–519.
- 31 B. H. Wilson, L. M. Abdulla, R. W. Schurko and S. J. Loeb, Translational dynamics of a non-degenerate molecular shuttle imbedded in a zirconium metal–organic framework, *Chem. Sci.*, 2021, **12**, 3944–3951.
- 32 E. Kimura, T. Shiota, T. Koike, M. Shiro and M. Kodama, A zinc(II) complex of 1,5,9-triazacyclododecane ([12]aneN3) as a model for carbonic anhydrase, *J. Am. Chem. Soc.*, 1990, **112**, 5805–5811.
- 33 M. H. Salter, J. H. Reibenspies, S. B. Jones and R. D. Hancock, Lewis Acid Properties of Zinc(II) in Its Cyclen Complex. The Structure of $[\text{Zn}(\text{Cyclen})(\text{SC}(\text{NH}_2)_2)](\text{ClO}_4)_2$ and the Bonding of Thiourea to Metal Ions. Some Implications for Zinc Metalloenzymes, *Inorg. Chem.*, 2005, **44**, 2791–2797.

